Article ID: 1006-8775(2017) 01-0081-10

SPATIO–TEMPORAL VARIATION OF ACTUAL EVAPOTRANSPIRATION AND ITS RELATION WITH CLIMATE PARAMETERS IN THE PEARL RIVER BASIN, CHINA

WU Ping (吴 萍)[1, 2, 3], LI Xiu-cang (李修仓)[2, 3], SU Bu-da (苏布达)[2, 3, 4], ZHAN Ming-jin (占明锦)[1, 5], WANG Yan-jun (王艳君)[2], JIANG Tong (姜 彤)[2, 3]

(1. Chinese Academy of Meteorological Sciences, Beijing 100081 China; 2. Collaborative Innovation Center on Forecast and Evaluation of Meteorological Disasters, Nanjing University of Information Science & Technology, Nanjing, 210044 China; 3. National Climate Center, China Meteorological Administration, Beijing 100081 China; 4. State Key Laboratory of Desert and Oasis Ecology, Xinjiang Institute of Ecology and Geography, Chinese Academy of Sciences, Urumqi 830011 China; 5. Jiangxi Province Climate Center, Nanchang 330046 China)

Abstract: Spatio-temporal variation of actual evapotranspiration (ETa) in the Pearl River basin from 1961 to 2010 are analyzed based on daily data from 60 national observed stations. ETa is calculated by the Advection-Aridity model (AA model) in the current study, and Mann-Kendall test (MK) and Inverse Distance Weighted interpolation method (IDW) were applied to detect the trends and spatial variation pattern. The relations of ETa with climate parameters and radiation / dynamic terms are analyzed by Person correlation method. Our findings are shown as follows: 1) Mean annual ETa in the Pearl River basin is about 665.6 mm/a. It has significantly decreased in 1961–2010 at a rate of –24.3 mm/10a. Seasonally, negative trends of summer and autumn ETa are higher than that of spring and winter. 2) The value of ETa is higher in the southeast coastal area than in the northwest region of the Pearl River basin, while the latter has shown the strongest negative trend. 3) Negative trends of ETa in the Pearl River basin are most probably due to decreasing radiation term and increasing dynamic term. The decrease of the radiation term is related with declining diurnal temperature range and sunshine duration, and rising atmospheric pressure as well. The contribution of dynamic term comes from increasing average temperature, maximum and minimum temperatures in the basin. Meanwhile, the decreasing average wind speed weakens dynamic term and finally, to a certain extent, it slows down the negative trend of the ETa.

Key words: complementary relationship theory; advection-aridity model; actual evapotranspiration; spatio-temporal variation; Pearl River basin

CLC number: P444 **Document code:** A

doi: 10.16555/j.1006-8775.2017.01.008

1 INTRODUCTION

In recent years, many studies found that both of the water surface evaporation [1-5] and the potential evapotranspiration [6-7] have been decreasing under the warming climate. This phenomenon is named as "Evaporation Paradox" because it is contradictory to the expected prediction. Many researchers have pointed out that the temperature is not the unique influencing parameter of evaporation, and believe that global dimming (decreasing solar radiation caused by increasing cloud cover and aerosols), declining wind speed, and decreasing daily temperature range might be the main reasons [1, 6, 8-10]. Based on the studies on the relationship between actual evapotranspiration (ETa) and pan evaporation (ETpan), Brutsaert and Parlange [11] concluded that ETpan decreases as a result of increasing ETa. Hobbins et al.[12] and Kahler et al.[13] also argue that there might be a complementary relationship between ETpan and ETa, because higher atmospheric water vapor, which hinders the evaporation of the water surface, has close positive relationship with ETa. Cohen et al. [9] concluded that complementary relationship restricts to arid areas. Ohmura and Wild[14] suggested that trends of ETpan can be used to make assumptions on the changing pattern of ETa.

Regional scale ETa studies are always dependent on model calculations due to limited reliable ETa observational data. Sun and Wu[15] have adopted coupled mode of land-atmosphere and simulated the surface evapotranspiration in Asia and North America; Liu et al. [16] studied the actual evapotranspiration in China by using the output from multiple land surface process models. To avoid the complexity of the soil-vegetation-atmosphere system, several researches[17-20] have conducted

Received 2015-02-03; **Revised** 2016-12-29; **Accepted** 2017-02-15

Foundation item: National Natural Science Foundation of China (41401056, 41571494); Research Innovation Program for College Graduates of Jiangsu Province (KYLX15_0858)

Biography: WU Ping, Ph. D. candidate, primarily undertaking research on climate change, hydrology and water resources.

Corresponding author: SU Bu-da, e-mail: subd@cma.gov.cn

contrast research on the actual evapotranspiration in Yellow River basin, Yangtze River basin and Haihe River basin by complementary relationship theory models using observed meteorological data. As for the Pearl River basin in South China, relevant researches mainly focus on pan evaporation and potential evapotranspiration[21-22], whereas researches on the actual evapotranspiration were much lacking.

The Pearl River basin, which is located between 116°E to 118°E and 20°N to 28°N, is the largest river system in South China with catchment area of about 690,000 km2 (Fig.1). The annual mean temperature ranges between 14℃ and 22℃, annual precipitation ranges between 1,200 mm and 2,200 mm [23-24]. With an annual quantity of 4,700 m^3 per capita (1.7 times of the n ational average), water resources in the basin is comparatively abundant. But water-related natural disasters such as floods, waterlogging, droughts, and groundwater salinization, etc, frequently threaten the sustainable development of regional social and economy [25-26]. The research on evapotranspiration plays high significance for understanding of the water cycle characteristics and water resources redistribution.

In the current study, the complementary theory based Advection-Aridity model (AA model) is adopted to deduce the actual evapotranspiration in the Pearl River basin on annual and seasonal scale for 1961 – 2010. The observed spatio-temporal changes of actual evapotranspiration in the basin are analyzed subsequently. The relation between ETa and climate parameters is analyzed in order to find key factors contributed highly to changing ETa. The findings from this study are expected to provide scientific information for the evaluation of the hydrologic cycle in the Pearl River basin, which enables an implementation of comprehensive water resources management strategy in South China.

2 DATA AND METHODOLOGY

2.1 *Data*

The daily meteorological record from 60 meteorological stations in the Pearl River basin has been obtained from the National Meteorological Information Center of China Meteorological Administration in Beijing. The dataset includes daily mean, maximum and minimum temperature, actual vapor pressure, sunshine duration, wind speed, etc. The available time period spans from 1961 to 2010. The data has been checked and controlled by homogeneity tests. River runoff data from eight hydrologic stations of associated sub-basins used for model calibration (1961 to 1990) is taken from the "China Hydrologic Year Book - the Pearl River basin volume". The distributions of the meteorological and hydrologic stations, as well as the sub-basins within the Pearl River basin are presented in Fig.1.

2.2 *The complementary relationship theory*

Bouchet [27] proposed a complementary relationship between actual and potential evapotranspiration in a wetting condition. He considered a regional scale uniform surface that involved characteristic scale of the order of 1 to 10 km. The potential evapotranspiration

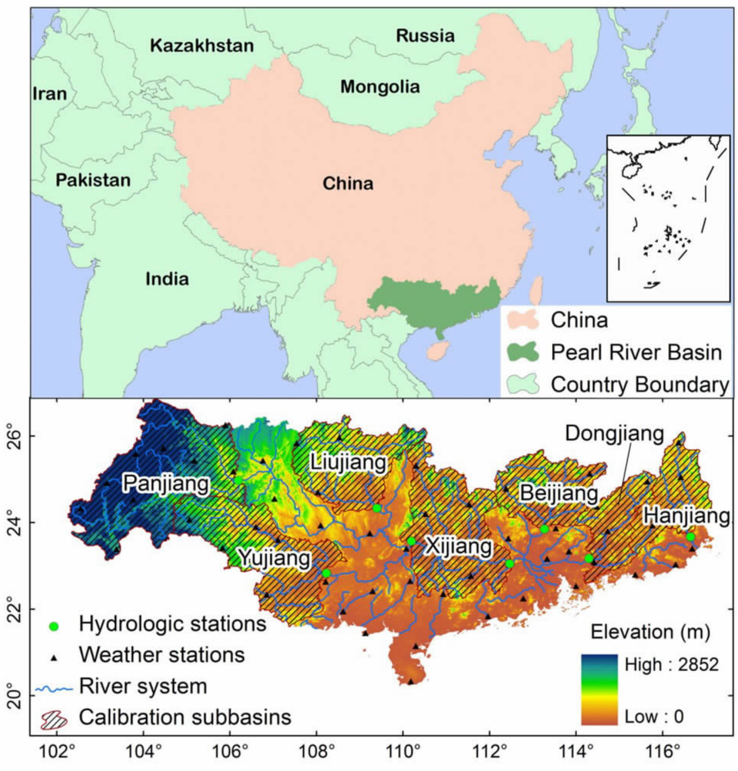

Figure 1. Distribution of climatic-hydrologic stations, tributaries, and sub-basins of the Pearl River basin.

(ETp) would take place if only the available energy were the limiting factor. ETw means the evapotranspiration in a wet environment. Then, under the circumstance of decreasing water supply (independent from available energy), ETa would decrease below ETw, and this decrease will have only a smaller impact on the net radiation than on temperature, humidity, and near-surface air turbulence. As a result, this available energy flux increases the ETp. According to the boundary thresholds of completely dry and completely wet conditions, the general equation of the complementary relationship can be expressed as:

$$\mathrm{ETa}+\mathrm{ETp}=2\mathrm{ETw} \tag{1}$$

where ETa is the actual evapotranspiration (mm), ETp is the potential evapotranspiration (mm), and ETw is the evapotranspiration, in a wet environment (mm).

The existence of a complementary relationship between ETa and ETp can be identified at 7 sub-basins in the Pearl River basin by calculating Eta and ETp with the water balance method and the Penman equation, respectively. Here, the annual precipitation is used to indicate the total water supply for every year. As shown in Fig.2, the existence of a complementary relationship between ETa and ETp is verified by an opposite trend of the two evapotranspiration parameters i.e. rising ETa and declining ETp in increasing annual precipitation conditions in the Pearl River basin.

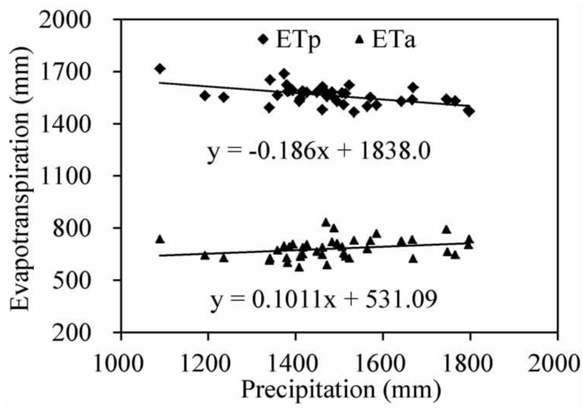

Figure 2. Identification of the complementary relationship between ETa and ETp in the Pearl River basin.

2.3 *Calculation and calibration of ETa with the Advection–Aridity model*

In recent years, several regional evapotranspiration models, such as the AA model [28], the Complementary Relationship Areal Evapotranspiration Model (CRAE Model)[29], and the Granger-Gray Model (GG Model) [30], have been widely used to estimate the ETa[31-34] theoretically. Among them, the AA model integrates fewer variables than the other models but proved to be providing higher accuracy in its calculation of ETa[21-23, 35-37]. The equations of the AA model are as follows:

$$\mathrm{ETa}=(2\alpha-1)\frac{\Delta}{\Delta+\gamma}(R_n-G)-\frac{\gamma}{\Delta+\gamma}E_a \tag{2}$$

$$\mathrm{ETp}=\frac{\Delta(R_n-G)}{\Delta+\gamma}+\frac{\gamma\cdot E_a}{\Delta+\gamma} \tag{3}$$

$$\mathrm{ETw}=\alpha\frac{\Delta(R_n-G)}{\Delta+\gamma} \tag{4}$$

where, Δ is the slope of the temperature-saturation vapor pressure curve (kPa·℃$^{-1}$); γ is the psychrometer constant (kPa·℃$^{-1}$); Rn is the surface net radiation (mm/day), with $R_n = R_{ns} - R_{nl}$; R_{ns} and R_{nl} being the net shortwave radiation and the net long wave radiation, respectively; E_a is the drying power (mm·d^{-1}); α is an empirical coefficient which is calibrated with the water balance method; and G is the soil heat flux (mm·d^{-1}); compared with the net radiation R_n, the soil heat flux G is small, especially when the surface is covered with vegetation and the time span is less than 10 days, thus G is set to zero in this study.

The net shortwave radiation R_{ns}, the net long wave radiation R_{nl} and the drying power E_a are calculated with the following equations[39]:

$$R_{ns}=(1-\alpha_R)\left(a_S+b_S\frac{n}{N}\right)\frac{24(60)}{\pi}G_{SC}d_r[\omega_S\sin(\varphi)\sin(\delta)+\cos(\varphi)\cos(\delta)\sin(\omega_S)] \tag{5}$$

$$R_{nl}=\sigma\left[\frac{T_{\max,K}{}^4+T_{\min,K}{}^4}{2}\right](0.34-0.14\sqrt{e_a})\left(1.35\frac{R_S}{R_{SO}}-0.35\right) \tag{6}$$

$$E_a=0.35(1+0.54U_2)(e_a^*-e_a) \tag{7}$$

In Eq. (5), α_R is the surface albedo, a_s and b_s are the transmission coefficients of extraterrestrial radiation, n is the sunshine duration and N is the longest possible sunshine duration, G_{sc} is the solar constant, d_r is the relative distance between the earth and the sun, ω_s is the sunset hour angle, φ is the latitude, and δ is the solar declination. In Eq. (6), σ is the Stephen-Boltzmann's constant, $T_{\max,K}$ and $T_{\min,K}$ are the highest and lowest daily temperatures (K), respectively, e_a is the actual water vapor pressure(kPa), and R_s/R_{so} is the relative shortwave radiation. In Eq. (7), u_2 is the wind speed at 2 m above ground (ms^{-1}), and e_a^* is the saturation water vapor pressure (kPa).

The empirical coefficient α in the AA model reflects the capacity of the transformation of the land surface energy Rn-G without advection into the latent heat flux, which is related to the condition of the underlying surface[40, 41]. Priestley and Taylor[38] proposed an average value of 1.26 for α, by using data of large-scale saturation land and ocean surface. In studies focusing on China, less accurate results have been obtained when α=1.26 is applied in the AA model. In general, α can be modified based on the regional water balance. For example, Mo [36] used α=1.08 when calculating ETa for the plain of north China, while Wang et al.[20] used α=1.01 in regions with an elevation above 500 m and α=1.105 in other regions of the Yangtze River basin. Li et al.[22] applied α=1.21 to the Haihe River basin. Considering the regional variation of α, here we calibrate α for 7 sub-basins in the Pearl

River basin respectively. Firstly, for each sub-basin, we set α change from 1.00 to 2.00 with a small step size $\Delta\alpha$ = 0.01, and calculate ETa for 100 times using the AA model. Secondly, the annual Eta was deduced based on the water balance model expressed as:

$$ETa=Pre-Run \quad (8)$$

where Pre indicates annual precipitation (mm) and Run is annual runoff (mm). This formula does not consider the annual changes of water storage in basins (such as agriculture irrigation and reservoir storage). Since most of hydraulic engineering in Pearl River basin was constructed in the later period of 1980s, water balance model based ETa in the calibration period (1961–1975) may have higher reliability. Errors may increase during validation period (1976–1990). We calculated annual proportion of water storage to annual precipitation in the Pearl basin (the area included Hainan Island and Hongshui River sub-basin) according to "Pearl River Water Resource Bulletin" in 2001–2011 (http://www.pearlwater. gov.cn /xxcx/szygg/) released by the Pearl River Water Conservancy Committee and found that the proportion is rather small (around ± 1%). Thus, it can be speculated that during calibration and verification periods without or with small-scale hydraulic engineering, it is acceptable to ignore the influence of water storage variable when calculating annual ETa using the water balance model. The locations of 7 calibrated sub-basins are shown in Fig.1 and the calibration results of α are listed in Table 1. It can be seen that after the calibration the relative error of the AA model is within ± 5% to the simple water balance model in all 7 sub-basins and hence shows a comparatively high accuracy.

Table 1. Calibration results of the AA model in the Pearl River basin.

Sub-basin	Hydrological station	Control area (km^2)	α	Simulation period (1961–1975) Annual mean ETa (mm)				Validation period (1976–1990) Annual mean ETa (mm)			
				Water balance	AA Model	Absolute error	Relative error	Water balance	AA Model	Absolute error	Relative error
Dongjiang	Boluo	25,441.5	**1.13**	819.7	831.9	12.2	1.5%	834.8	807.3	-27.5	-3.3%
Hanjiang	Chaoan	29,045.1	**1.04**	666.4	657.2	–9.2	–1.4%	642.0	639.3	-2.7	-0.4%
Xijiang	Gaoyao	62,970.3	**1.11**	774.0	764.7	–9.3	–1.2%	729.1	747.5	18.4	2.5%
Beijiang	Hengshi	33,902.2	**1.00**	513.8	537.5	23.6	4.6%	518.1	502.1	-15.9	-3.1%
Liujiang	Liuzhou	45,426.1	**1.11**	676.8	681.0	4.2	0.6%	706.9	674.1	-32.9	-4.6%
Yujiang	Nanning	62,362.1	**1.04**	639.8	643.3	3.4	0.5%	618.7	632.6	13.9	2.2%
Nanbeipanjiang	Zhexiang	86,143.8	**1.13**	691.8	680.7	–11.1	–1.6%	650.3	677.4	27.1	4.2%
Other regions		345,291.2	**1.09**	–	–	–	–	–	–	–	–

Note: "Other regions" are the regions which are not calibrated based on the water balance model; the value of α in such regions is calculated from the α values of the seven sub-basins by the area-weighted average method.

2.4 *Statistical methods*

Annual and seasonal trends are detected by the linear regression method, while the non-parametric Mann-Kendall test[42] is used to detect the significance of the trend. The areal amounts of precipitation and ETa are calculated based on the Thiessen polygon method[43]. The spatial distribution of the ETa was interpolated by the inverse distance weighted (IDW) method [44]. The detailed relationship of the variables is analyzed with the Pearson coefficient of association [45], and the significance of the relationship is determined at the 0.05 and 0.01 level.

3 SPATIO–TEMPORAL VARIATION OF ETA

3.1 *Temporal variation of ETa*

According to the ETa from calibrated AA model for 60 meteorological stations in the Pearl River basin from 1961 to 2010, multi-year averaged annual ETa is 665.6 mm. About 232.6 mm for summer, 184.1 mm for autumn, 103 mm for winter, and about 146.3 mm for spring are calculated. In Fig.3, the inter-annual and seasonal variation of ETa in the Pearl River basin is visualized for 1961–2010. It can be seen that the annual ETa shows significant decreasing trend at a rate of about –24.3 mm per decade (at 0.01 significance level), and seasonal time series also shows similar decreasing trends with winter ETa having the least significance level of 0.1. The seasonal ETa tendencies are estimated at –4.3 mm, –10.4 mm, –8.2 mm, and –1.5 mm per decade for spring, summer, autumn, and winter, respectively.

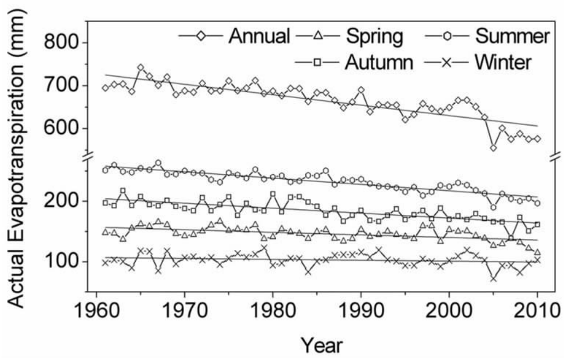

Figure 3. Annual and seasonal variation of ETa in the Pearl River basin from 1961 to 2010.

The decadal variation of seasonal ETa is presented in Table 2. In general, summer and autumn ETa have shown a steady downward trend, and the decreasing scope is the maximum in the 1990s, with rate of −6.9% (summer) and −6.4% (autumn) compared with previous decade, respectively. However in winter, an increase by 3.6% occurred in the 1970s followed by a steady decline with a value around 98.4 mm in the 2000s. In Spring, ETa also shows sustained decrease, but a little break of about 0.8% increment was found in the 1990s.

Table 2. Decadal variation of ETa in the Pearl River basin.

Decade	Spring		Summer		Autumn		Winter	
	(mm)	(%)	(mm)	(%)	(mm)	(%)	(mm)	(%)
1960s	152.5	-	251.8	-	197.6	-	103.3	-
1970s	152.2	-0.2	241.9	-3.9	193.2	-2.2	107.0	+3.6
1980s	145.5	-4.4	237.8	-1.7	188.2	-2.6	104.7	-2.2
1990s	146.7	+0.8	221.5	-6.9	176.1	-6.4	101.8	-2.7
2000s	134.8	-8.1	209.7	-5.3	165.3	-6.1	98.4	-3.4
Average	146.3	-3.0	232.6	-4.5	184.1	-4.4	103.0	-1.2

Notes :The 1960s cover the period 1961-1970, etc.

3.2 *Spatial distribution of average ETa*

Spatial distribution of annual and seasonal mean ETa in the Pearl River basin are shown in Fig.4. Highest annual ETa, with values above 800 mm can be founded at the river delta and the eastern part of the basin. These two regions are located in the downstream region of the Xijiang River sub-basin and the upper reaches of the Dongjiang River sub-basin. Two regions of low ETa are situated in the central western region and the northeastern part. The ETa shows a large spatial disparity from below 600 mm in the western to more than 800 mm in the eastern part of the center. Similar

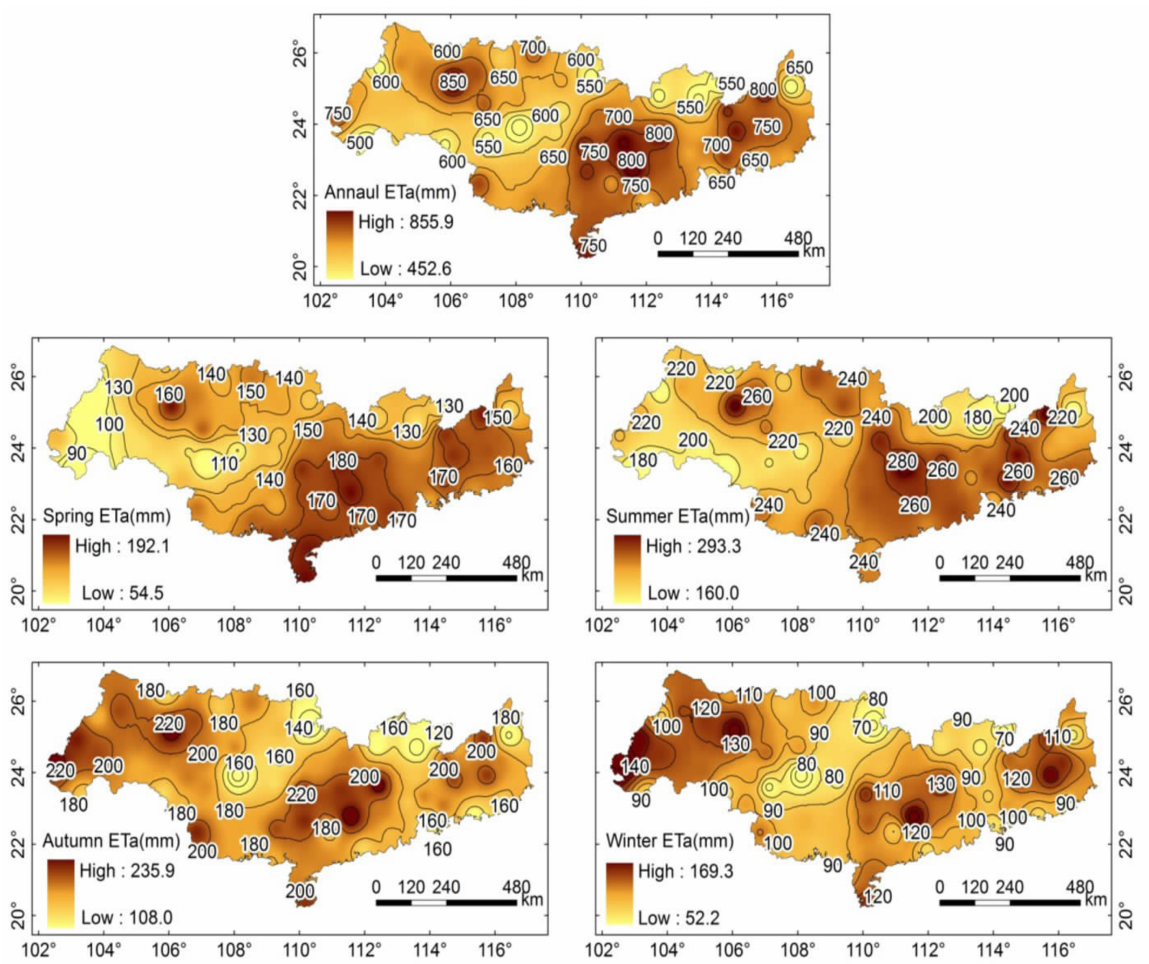

Figure 4. Spatial distribution of mean annual and seasonal ETa in the Pearl River basin in 1961-2010.

findings are found for the seasonal distribution. For all seasons, particularly spring and summer, ETa has the highest values in the eastern part of the basin, while in autumn and winter high values of ETa are also found in the western part. Low ETa values are obviously in the central west and northeast of the basin.

From 1961 to 2010, significant decreasing trends of annual and seasonal ETa can be found in the most parts of the basin (Fig.5). At only fewer stations located in the central western part, the annual ETa is significantly increasing. Similar pattern is detected for summer, and autumn, where again none or slightly increasing trends are found in the middle of the basin. The spatial distribution of trends for spring and winter are different from summer and autumn, as only few significant trends are found throughout the basin.

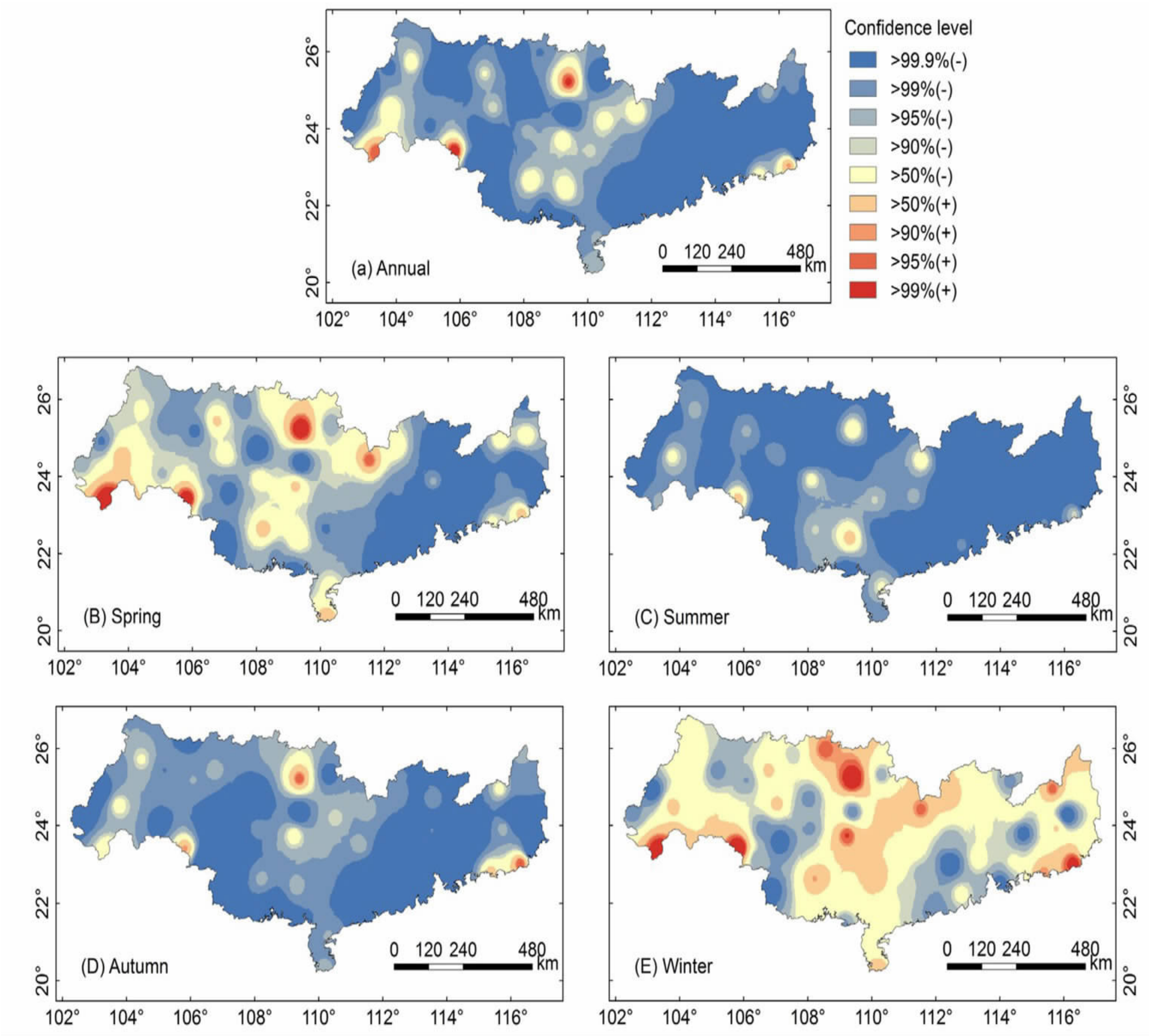

Figure 5. Spatial distribution of annual and seasonal ETa trends in the Pearl River basin, 1961-2010.

4 REASONS OF DECREASING ETA

4.1 *Causes of spatio-temporal variation of ETa*

In general, it is assumed that the decreasing ETa is mainly caused by the changes of both climatic and geographical parameters. Based on the AA model's structure, the spatio-temporal changes of ETa are mainly caused by two elements including the radiation term and the dynamic term. ETa has a positive correlation with the radiation term, but a negative correlation with the dynamic term. Besides, the α value varies by sub-basins and is affected by the surface water supply. In Table 3, the two model elements and their associated climatic and geographical parameters in the Pearl River basin are summarized. As the geographical parameters such as latitude and elevation, are constants, ETa variation is mainly caused by climatic parameters. Therefore, in the following section, we will analyze the correlation between climate parameters and two model elements for detecting the contribution of climatic parameters to ETa.

Table 3. Climatic and geographical parameters affecting to ETa.

Model elements	Equation	Meteorological and geographical parameters
Radiation term	$\frac{\Delta}{\Delta+\gamma}(R_n-G)$	(1) The slope of saturated vapor pressure curve (Δ): Mean Temperature (Tmean) (2) The psychrometer coefficient (γ): Atmospheric pressure (P) (3) Net radiation (Rn): Max, Minimum Temp. (Tmax, Tmin); Actual vapor pressure (ea); Sunshine duration (Sun); latitude (φ); Elevation (Alt)
Dynamic term	$\frac{\gamma}{\Delta+\gamma}E_\alpha$	(1) The saturated vapor pressure of slope (Δ): Mean Temperature (Tmean) (2) The psychometric coefficient (γ): Atmospheric pressure (P) (3) Drying power (Ea): wind speed (u2); Mean Temperature (T); Actual vapor pressure (ea)
α	ETa = Pre - Run	(1) Precipitation (Pre)

Table 4. Pearson correlation coefficients and trend statistic between the main meteorological parameters and the radiation / dynamic term.

	Element / Trend	Tmean	Tmax	Tmin	Trange	Air Pressure (P)	Actual vapor pressure (ea)	Sunshine Duration (Sun)	Wind Speed (u2)	Trend
Annual	Radiation term	-0.238	0.085	-0.482**	0.794**	-0.422**	-0.112	0.922**	\	-0.728**
	Dynamic term	0.300*	0.523**	0.120	0.552**	-0.190	-0.439**	\	0.257	0.169
	Trend	0.607**	0.412**	0.722**	-0.447**	0.495**	-0.038	-0.586**	-0.697**	\
Spring	Radiation term	0.560**	0.709**	0.318*	0.853**	-0.344*	0.420**	0.957**	\	-0.543**
	Dynamic term	0.557**	0.683**	0.349*	0.763**	-0.329*	0.114	\	0.600**	-0.162
	Trend	0.181	0.057	0.353*	-0.379**	0.477**	-0.096	-0.459**	-0.756**	\
Summer	Radiation term	0.041	0.291*	-0.362**	0.757**	-0.371**	-0.091	0.962**	\	-0.665**
	Dynamic term	0.757**	0.783**	0.556**	0.375**	0.058	-0.347*	\	0.443**	0.449**
	Trend	0.572**	0.380**	0.758**	-0.348*	0.478**	-0.086	-0.536**	0.051	\
Autumn	Radiation term	0.068	0.386**	-0.194	0.645**	-0.246	-0.038	0.851**	\	-0.502**
	Dynamic term	0.045	0.366**	-0.227	0.660**	0.110	-0.713**	\	0.187	0.342*
	Trend	0.469**	0.394**	0.444**	-0.060	0.488**	-0.148	-0.232	-0.353*	\
Winter	Radiation term	0.490**	0.753**	0.224	0.833**	-0.114	0.266	0.882**	\	-0.241
	Dynamic term	-0.053	0.188	-0.232	0.604**	-0.260	-0.432**	\	0.286*	-0.136
	Trend	0.413**	0.250	0.521**	-0.338*	0.500**	0.213	-0.265	-0.691**	\

Notes：* indicates the correlation passes the 0.05 level significant test; ** indicates the correlation passes the 0.01 level significant test.

4.2 *Relationship among radiation term, dynamic term and climatic parameters*

In order to identify causes of the spatio-temporal variation of ETa, the climatic parameters are correlated with radiation term and dynamic term. Table 4 shows the Pearson correlation coefficients between the annual/seasonal meteorological parameters and the values of the annual and seasonal radiation term and the dynamic term, respectively.

At the annual scale, significant positive correlations are found between the radiation term and the diurnal temperature range (daily maximum temperature minus daily minimum temperature) as well as sunshine duration. Significant negative correlations are found between the annual radiation term and the minimum temperature and atmospheric pressure. There are significant positive correlations between the dynamic term and the average temperature as well as the diurnal temperature, while there is a significant negative correlation between the dynamic term and the actual vapor pressure. In summer, the radiation term correlates positively with the maximum temperature, diurnal temperature range and sunshine duration, but negatively with the minimum temperature and air pressure. The dynamic term correlates positively with the maximum and minimum temperature, diurnal temperature range and wind speed, but negatively with the air pressure. In autumn, the radiation term correlates only positively with the maximum temperature, diurnal temperature range, and sunshine duration. The dynamic term correlates positively with the maximum temperature and diurnal temperature range, but negatively with the actual vapor pressure.

The annual and seasonal trends of meteorological parameters (Table 4) show that at annual, summer and autumn the radiation term is decreasing, but the dynamic term is increasing. The different positive and negative seasonal trends of dynamic term result in a lower significance of the association with the ETa changes. It is apparent that the decreasing ETa in the Pearl River basin can be related with these decreases in the radiation term and increases in the dynamic term. Furthermore, changes in ETa can be particularly attributed to simultaneous increases of the average, maximum, minimum temperature, and air pressure, and decreases of the diurnal temperature range, sunshine duration, and wind speed. Apparently, decreasing diurnal temperature range and sunshine duration as well as increasing air pressure cause the radiation term to decrease, while increasing average, maximum, and minimum temperature mainly cause the dynamic term to increase.

5 CONCLUSION AND DISCUSSION

In the current paper, complementary relationship theory based Advection-Aridity model is applied to calculate the actual evapotranspiration (ETa) for the Pearl River basin. The spatio-temporal variation of ETa is analyzed by applying the Mann-Kendall test and the Inverse Distance Weighted interpolation method, and the Pearson correlation method is used to analyze the relationship between meteorological parameters and the radiation / dynamic term. Following major results are obtained:

(1) The annual ETa of the Pearl River basin is about 665.6 mm. A significant negative trend has been detected for the entire study period of 1961–2010, with a decreasing rate of 24.3 mm per decade. The negative trend of seasonal ETa is more significant in summer and autumn than in winter and spring.

(2) The amount of annual ETa is higher in the southeast coastal area than in the northwestern region of the Pearl River basin. Except for few stations in the central west region and the northeast region, significant decreasing trends of ETa are found in most parts of the basin.

(3) Our study found that the decreasing ETa in the Pearl River basin can be explained by decreased radiation term and/or increased dynamic term. The decrease of the diurnal temperature range and sunshine duration and the increase of the atmospheric pressure caused declining radiation term and then induced ETa decrement. In addition, the increase of average/maximum/minimum temperature in the basin contributed more to the increasing dynamics term rather than the radiation term, so the final impact is to accelerate ETa decrement. Meanwhile, the weakening of average wind speed caused the decrease of the dynamic term and which in turn, slowed down the declining trend of ETa.

Gao et al. [46] found a similar decreasing trend of ETa in South China by using a modified water balance model. The similar findings prove that the complementary relationship based AA model is suitable for application in South China, which is also supported by the findings from Xu and Singh[23] for temperate humid regions. The major advantage of application of the AA model is that it can depend only on the meteorological parameters to calculate ETa. This is very beneficial for regions with comparatively dense meteorological observation network. A major obstacle lies in the process of α calibration, which is calibrated and adjusted by the water balance model, and depends on the surface water supply conditions which are mainly controlled by precipitation amounts. Although only meteorological parameters are needed for the AA model, the validation is still dependent on the hydrological runoff data for the calculation of the water balance model. In China, calibrations of α, on regional or local scale, necessitate the availability of long-term runoff data. Once α has been calibrated on a sub-basin scale for Chinese river basins, the continuous use of the AA model for the calculation of past and future actual evapotranspiration can be facilitated.

REFERENCES:

[1] PETERSON T, GOLUBEV V, GROISMAN P. Evaporation losing its strength [J]. Nature, 1995, 337 (6551): 687-688.
[2] RODERICK M, FARQUHAR G. The cause of decreased pan evaporation over the past 50 years [J]. Science, 2002, 298 (5597): 1410-1411.
[3] Roderick M, HOBBINS M, FARQUHAR G. Pan Evaporation Trends and the Terrestrial Water Balance. I. Principles and Observations [J]. Geography Compass, 2009, 3(2): 746-760, 10.1111/j.1749-8198.2008.00213.x.
[4] WANG Yan-jun, JIANG Tong, XU Chong-yu. Observed trends of Pan Evaporation and its impact factors over the Yangtze River basin between 1961 and 2000 [J]. J Nat Resour. 2005, 20(6): 864-870 (in Chinese).
[5] ZENG Yan, QIU Xin-fa, LIU Chang-ming, et al. Changes of Pan Evaporation in China in 1960-2000 [J]. Adv Water Sci, 2007, 18(3): 311-318 (in Chinese).
[6] CHATTOPADHYAY N, HULME M. Evaporation and potential evapotranspiration in India under conditions of recent and future climate change [J]. Agricult Forest Meteorol, 1997, 87(1): 55-73.
[7] GAO Ge, CHEN De-liang, REN Guo-yu, et al. Trend of potential evapotranspiration over China during 1956 to 2000 [J]. Geograph Res, 2006, 25(3): 378-387.
[8] REN Guo-yu, GUO Jun. Change in Pan Evaporation and the influential factors over China: 1956-2000 [J]. J Nat Resour, 2006, 21(1): 31-44 (in Chinese).
[9] COHEN S, IANETZ A, STANHILL G. Evaporative climate changes at Bet Dagan, Israel, 1964-1998 [J]. Agricult Forest Meteorol, 2002, 111(2): 83-91.
[10] CONG Zhen-tao, NI Guang-heng, YANG Da-wen, et al. Evaporation paradox in China [J]. Adv Water Sci, 2008, 19(2): 147-152.
[11] BRUTSAERT W, PARLANGE M. Hydrologic cycle explains the evaporation paradox [J]. Nature, 1998, 396

(6706): 30-31.
[12] HOBBINS M, RAMIREZ J, BROWN T. Trends in pan evaporation and actual evapotranspiration across the conterminous U.S.: Paradoxical or complementary? [J]. Geophys Res Lett, 2004, L13 503(31): 1-5.
[13] KAHLER D, BRUTSAERT. Complementary relationship between daily evaporation in the environment and pan evaporation [J]. Water Resour Res, 2006, W05413(42), doi: 10.1029/2005WR004541.
[14] OHMURA A, WILD M. Is the hydrological cycle acceleration? [J]. Science, 2002, 298(5597): 1345-1346. doi: 10.1126/science.1078972.
[15] SUN Lan, WU Guo-xiong. The impact of territorial evapotranspiration on climate change. Science in China (Series D). 2001, 31(1): 59-69 (in Chinese).
[16] LIU Bo, XIAO Zi-niu, MA Zhu-guo. Relationship between pan evaporation and actual evaporation in different humid and arid regions of China [J]. Plateau Meteorol, 2010, 29(3): 629-636 (in Chinese).
[17] QIU Xin-fa, ZENG Yan, MIAO Qi-long, et al. Estimation of annual actual evapotranspiration from nonsaturated land surfaces with conventional meteorological data [J]. Sci China (Ser D), 2004, 47(3): 239-246.
[18] ZENG Yan. Distributed Modeling of Actual Evapotranspiration over Rugged Terrian of Yellow River Basin [D]. Ph. D. Thesis, Institute of Geographic Sciences and Natural Resources Research, Beijing, 123 pp. 2004 (in Chinese).
[19] WANG Yan-jun, LIU Bo, SU Bu-da, et al. Trends of Calculated and Simulated Actual Evaporation in the Yangtze River Basin [J]. J Climate, 2011, 24 (8): 4494-4507.
[20] LI Xiu-cang, GEMMER M, ZHAI Jian-qing, et al. Spatio-temporal variation of actual evapotranspiration in the Haihe River Basin of the past 50 years [J]. Quatern Int, 2013, 304: 133-141.
[21] XIAO Wei-jun, LIANG Yu-qiong, HE Ju-xiong, et al. Spatial and temporal variations of evaporation over south China in autumn [J]. J Trop Meteorol, 2008, 14(2): 157-160.
[22] DING Ju-li, FEI Jian-fang, HUANG Xiao-gang, et al. Improvement to the evaporation duct model by introducing nonlinear similarity functions in stable conditions [J]. J Trop Meteorol, 2011, 17(1): 64-72.
[23] FAN Shao-jia, WANG An-Yu, FAN Qi, et al. Atmospheric boundary layer concept model of the Pearl River Delta and its application [J]. J Trop Meteorol, 2007, 13(1): 8-13.
[24] JIAN Mao-qiu, QIAO Yun-ting, HUANG Wei et al. The variation of evaporation over South China and its relationships to precipitation [J]. J Trop Meteorol, 2011, 17(3): 285-292.
[25] FISCHER T, GEMMER M, SU B, et al. Hydrological long-term dry and wet periods in the Xijiang River Basin, South China [J]. Hydrol Earth Sys Sci, 2013, 17 (1): 135-148.
[26] LI Jiang-nan, YE Ai-fen, XU Yong-hui, et al. Evolution of moist potential vorticity during a warm-zone heavy rainfall event in the Pearl River Delta [J]. J Trop. Meteorol, 2011, 17(3): 310-316.
[27] BOUCHET R. Evapotranspiration réelle et potentielle, signification climatique [C]// International Association of Hydrological Sciences Publication: Proceedings of General Assembly, Berkeley, California Symposium. 1963: 134-142.
[27] PENMAN H. Natural evaporation from open water, bare soil and grass [J]. Proceedings of the Royal Society of London, Series A, Mathematical and Physical Sciences, 1948, 193(1032): 120-145.
[28] BRUTSAERT W, STRICKER H. An advection-aridity approach to estimate actual regional evapotranspiration [J]. Water Resour Res, 1979, 15(2): 443-450
[29] MORTON F. Operational estimates of areal evapotranspiration and their significance to the science and practice of hydrology [J]. J Hydrol, 1983, 66(1): 1-76.
[30] GRANGER R, GRAY D. Evaporation from natural nonsaturated surfaces[J]. J Hydrol, 1989, 111(1): 21-29.
[31] SHANG Song-hao, SUN Li-yan, HAO Zeng-chao. Using Complementary Relationship to Estimate Monthly Evapotranspiration in Arid Oasis [J]. J China Hydrol, 2008, 28(3): 67-39. (in Chinese).
[32] HAN Song-jun, HU He-ping, TIAN Fu-qiang. Evaluation of applicability of three evapotranspiration models using meteorological data [J]. J Hydraul Engineer. 2009, 40(1): 75-81 (in Chinese).
[33] LIU Jian, ZHANG Qi, XU Chong-yu, et al. Change of actual evapotranspiration of Poyang Lake watershed and associated influencing factors in the past 50 years [J]. Resour Environ Yangtze Basin, 2010, 19(2): 139-145 (in Chinese).
[34] ZHAI Lu-xin, FENG Qi, LI Yi, et al. Calculation of actual evapotranspiration based on Morton CRAE in Northwest China [J]. J Irrig Drain, 2010, 29 (5): 33-38. (in Chinese).
[35] WANG Yan-jun, JIANG Tong, LIU Bo. Trends of estimated and simulated actual evapotranspiration in the Yangtze River Basin [J]. Acta Geograph Sinica, 2010, 65 (9): 1079-1088 (in Chinese).
[36] Mo Xing-guo. An advection-Aridity evaporation model for wheat field evapotranspiration and advection [J]. Chin J Agrometeorol, 1995, 16(6): 1-4 (in Chinese).
[37] HOBBINS M, RAMIREZ J. The complement relationship in estimation of regional evapotranspiration: An enhanced Advection-Aridity model [J].Water Resour Res, 2001, 37 (5): 1389-1403.
[38] PRIESTLEY C, TAYLOR R. On the assessment of surface heat flux and evaporation using large-scale parameters [J]. Mon Wea Rev, 1972, 100(2): 81-92.
[39] ALLEN R, PEREIRA L, RAES D, et al. Crop evapotranspiration guidelines for computing crop water requirements [M]// FAO Irrigation and Drainage Paper 56. Food and Agriculture Organization of the United Nations, 1998, Rome, Italy.
[40] EAGLESON P. Ecohydrology: Darwinian Expression of Vegetation Form and Function [M]. Cambridge: Cambridge University Press, 2002.
[41] YANG Han-bo, YANG Da-wen, LEI Zhi-dong, et al. 2008. Regional variability of the complementary relationship between actual and potential evapotranspiration [J]. J Tsinghua Univ (Sci & Tech). 48 (9): 1413-1416 (in Chinese).
[42] LU Hong, CHEN Si-rong, Guo Yuan, et al. Spatio-temporal variation characteristics of extremely heavy precipitation frequency over South China in the

last 50 Years [J]. J Trop Meteorol, 2014, 20(3): 279-288.
[43] HARTKAMP A, BEURS K, STEIN A, et al. Interpolation Techniques for Climate Variables [M]. NRG-GIS Series 99-01, Mexico, D.F.: CIMMYT, 1999: 1-26.
[44] GEMMER M, BECKER S, JIANG Tong. Observed monthly precipitation trends in China 1951-2002 [J]. Theor Appl Climatol, 2004, 77(1) 39-45.
[45] WU Wei, WEN Zhi-ping, CHEN Yun-guang, et al. Interannual variability of winter and spring precipitation in South China and its relation to moisture transport [J]. J Trop Meteorol, 2013, 19(4): 322-330.
[46] GAO Ge, CHEN De-liang, XU Chong-yu, et al. Trend of estimated actual evapotranspiration over China during 1960-2002 [J]. J Geophys Res, 2007, 112, D11120, doi: 10.1029/2006JD008010.

Citation: WU Ping, LI Xiu-cang, SU Bu-da et al. Spatio-temporal variation of actual evapotranspiration and its relation with climate parameters in the Pearl River basin, China [J]. J Trop Meteorol, 2017, 23(1): 81-90.